

Oncomodulin, an EF-Hand Ca^{2+} Buffer, Is Critical for Maintaining Cochlear Function in Mice

Benton Tong,¹ Aubrey J. Hornak,² Stéphane F. Maison,³ Kevin K. Ohlemiller,¹ M. Charles Liberman,³ and Dwayne D. Simmons²

¹Department of Otolaryngology, Washington University School of Medicine, St. Louis, Missouri 63110, ²Department of Integrative Biology and Physiology, University of California, Los Angeles, Los Angeles, California 90095, and ³Eaton–Peabody Laboratory, Massachusetts Eye and Ear Infirmary, and Department of Otology and Laryngology, Harvard Medical School, Boston, Massachusetts 02114

Oncomodulin (Ocm), a member of the parvalbumin family of calcium binding proteins, is expressed predominantly by cochlear outer hair cells in subcellular regions associated with either mechanoelectric transduction or electromotility. Targeted deletion of Ocm caused progressive cochlear dysfunction. Although sound-evoked responses are normal at 1 month, by 4 months, mutants show only minimal distortion product otoacoustic emissions and 70–80 dB threshold shifts in auditory brainstem responses. Thus, Ocm is not critical for cochlear development but does play an essential role for cochlear function in the adult mouse.

Key words: calcium homeostasis; hearing loss; outer hair cell; parvalbumin

Significance Statement

Numerous proteins act as buffers, sensors, or pumps to control calcium levels in cochlear hair cells. In the inner ear, EF-hand calcium buffers may play a significant role in hair cell function but have been very difficult to study. Unlike other reports of genetic disruption of EF-hand calcium buffers, deletion of oncomodulin (Ocm), which is predominately found in outer hair cells, leads to a progressive hearing loss after 1 month, suggesting that Ocm critically protects hearing in the mature ear.

Introduction

Because Ca^{2+} has roles in mechanoelectric transduction, cochlear amplification, and synaptic function (Zhang et al., 2003; Stepanyan and Frolenkov 2009; Pangršič et al., 2015), the regulation and control of Ca^{2+} is a major challenge for cochlear hair cells. The mammalian cochlea has two types of hair cells involved in the transduction of sound into electrical responses. Outer hair cells (OHCs) amplify vibrations of the cochlear partition directly enhancing sensitivity and frequency selectivity, whereas the inner hair cells (IHCs) release glutamate from ribbon synapses directly exciting the endings of auditory nerve fibers responsible for transmitting sound information to

the brain. The OHCs are prominent targets of noise and aging and, when damaged, lead to elevated hearing thresholds and loss of cochlear frequency tuning.

To control Ca^{2+} levels in hair cells, a multitude of proteins act as buffers, sensors, or pumps. Although previous studies show that the free Ca^{2+} concentration in OHCs rises after acoustic overstimulation (Fridberger et al., 1998), there are few studies that link Ca^{2+} homeostasis directly with hearing loss (Mammano 2011). In hair cells, mobile EF-hand Ca^{2+} -binding proteins or “buffers” may play a significant role in Ca^{2+} homeostasis and signaling. These proteins are characterized by a common sequence of ~30 residues forming a helix–loop–helix motif, which, when bound to Ca^{2+} , causes a conformational change, allowing for interaction with downstream proteins (Lewit-Bentley and Réty 2000). Although most EF-hand Ca^{2+} buffers are found extensively throughout the nervous system, oncomodulin (Ocm), an isoform of α -parvalbumin originally discovered in a rat hepatoma (MacManus et al., 1983), is limited to OHCs and also found in macrophages (Thalmann et al., 1998; Yang et al., 2004; Yin et al., 2009). In the inner ear, mobile EF-hand Ca^{2+} buffers have been difficult to study, because their expression levels change during maturation (Pack and Slepecky 1995; Sage et al., 2000). For example, α -parvalbumin, calretinin, and calbindin-D28k are expressed in both IHCs and OHCs at birth and are all downregulated in OHCs, whereas Ocm is upregulated before the onset of hearing (Pack and

Received Sept. 1, 2015; revised Dec. 16, 2015; accepted Dec. 22, 2015.

Author contributions: D.D.S. designed research; B.T., A.J.H., S.F.M., K.K.O., and D.D.S. performed research; M.C.L. and D.D.S. contributed unpublished reagents/analytic tools; M.C.L. and D.D.S. analyzed data; D.D.S. wrote the paper.

We thank the Mouse ES and Mouse Genetics Cores at Washington University and University of California, Los Angeles, and Drs. R. Thalmann, I. Thalmann, and D. Ornitz (Washington University) for their advice and technical assistance. We also acknowledge Dr. C.-L. Hseh for karyotyping and the Washington University Mouse Genetics Core for injection services. This research was supported by National Institute on Deafness and Other Communication Disorders Grants DC004086 and DC013304 (D.D.S.) and R01 DC00188 and P30 DC05209 (M.C.L.), and a 2015–2016 Fulbright Scholar Award (D.D.S.).

The authors declare no competing financial interests.

Correspondence should be addressed to Dwayne D. Simmons, Department of Integrative Biology and Physiology, University of California, Los Angeles, Los Angeles, CA 90095. E-mail: dd.simmons@ucla.edu.

DOI:10.1523/JNEUROSCI.3311-15.2016

Copyright © 2016 the authors 0270-6474/16/361631-05\$15.00/0

Slepecky 1995; Yang et al., 2004; Simmons et al., 2010). In OHCs, the possible replacement of multiple Ca^{2+} buffers by a single one, Ocm, suggests its functional specificity in OHCs. Estimates from immunogold studies suggest that Ocm levels may be as high as 4–6 mM in OHCs (Hackney et al., 2005). In the mouse ear, Ocm is preferentially localized to subcellular compartments associated with Ca^{2+} -dependent motility processes, i.e., along the sides of the OHCs, above the synaptic zone, and below the cuticular plate in which the stereocilia insert (Simmons et al., 2010). Given that Ocm is a member of the parvalbumin family, is subcellularly compartmentalized, and is prominent in OHCs to the exclusion of other EF-hand Ca^{2+} buffers, its role in the regulation of Ca^{2+} may be critically important to OHC function (Hackney et al., 2005; Simmons et al., 2010).

To test our ideas about the importance of OHC Ca^{2+} buffering in general, and Ocm specifically, we engineered a targeted deletion of Ocm. Previous studies of genetic disruption of α -parvalbumin, calbindin-D28k, and calretinin have not reported any inner ear phenotype for either individual or combined knock-outs of these EF-hand Ca^{2+} buffers (Airaksinen et al., 2000; Pangršič et al., 2015).

Materials and Methods

All experiments were done in compliance with National Institutes of Health and institutional animal care guidelines and were approved by the following institutional animal care and use committees: University of California, Los Angeles, Massachusetts Eye and Ear Infirmary, and Washington University School of Medicine.

Generation of Ocm mutant mice. The coding sequence for mouse Ocm is contained in five exons on chromosome 5 (Staubli et al., 1995). Seventeen kilobases of the Ocm gene containing exons 2–4 were cloned into pBSKS from BAC DNA. As illustrated in Figure 1A, a LoxP site was engineered 5' of exon 2, and an F₁p-neo-F₁p-LoxP cassette was engineered 3' of exon 4. After sequencing of the exon junctions, the 5' LoxP site and the 3' cassette, the vector was electroporated into ES cells (SSC#10, 129sv), and clones resistant to G418 were isolated (electroporation and selection of resistant clones was done at the Washington University Embryonic Stem Cell Core) and checked for homologous recombination by Southern blot analysis. Positive clones were karyotyped. Two male clones were injected into C57BL/6J blastocysts. High percentage chimeras were crossed with CBA/CaJ mice, and the pups were checked for germ-line transmission. Initial confirmation of germ-line transmission was done by Southern blot analysis. Subsequently, PCR primers used for genotyping were made from the deleted region (5'-CTC CAC ACT TCA CCA AGC AG-3' and 5'-GCT TGG GGA CCC CCT GTC TTC A-3') and from the targeting vector (5'-CTC CAC ACT TCA CCA AGC AG-3' and 5'-TTT CAT GTT CAG GGA TCA AGT G-3'). The neo gene was removed when generating the Ocm heterozygote to avoid any possible interference (Wassarman et al., 1997). Two Ocm heterozygote (*Ocm*^{flox/+}) mutants were crossed to generate an Ocm homozygote flox (*Ocm*^{flox/flox}) mutant. The *Ocm*^{flox/flox} mouse was crossed with a mouse line with Cre recombinase under the control of the β -actin promoter (strain 003376; The Jackson Laboratory) to generate *Actb*^{Cre}; *Ocm*^{flox/flox} mice (*Ocm*^{tm1.1Ddsi}, MGI:97401).

Functional and morphological assays. For *in vivo* functional assays, mice were anesthetized with ketamine (100 mg/kg, i.p.) and xylazine (10 mg/kg, i.p.) and were maintained at a body temperature of 37°C during testing. Auditory brainstem responses (ABRs) and distortion product otoacoustic emissions (DPOAEs) were measured as described previously (Ohlemiller et al., 2011; Maison et al., 2012). For histological analysis and immunocytochemistry, anesthetized mice were perfused transcardially with 4% paraformaldehyde in 0.1 M phosphate buffer. Cochleae were prepared as cochlear whole mounts or mid-modiolar sections as described previously (Simmons et al., 2010; Maison et al., 2012). For whole mounts, each cochlea was microdissected and immunostained with antibodies to myosin VIIa (1:200, rabbit polyclonal; Proteus Biosciences) and appropriate secondary antibodies. Whole mounts were further stained with phalloidin. For mid-modiolar sections, cochleae were embedded in a gelatin-agarose solution, and 200 μm vibratome sections

were taken and immunostained with antibodies to α -parvalbumin (1:2000, goat polyclonal; PVG-214; Swant) or calretinin (1:500, goat polyclonal; CG1; Swant) and prestin (1:1000, rabbit polyclonal; kind gift from R. Fettiplace, University of Wisconsin, Madison, WI). Confocal z-stacks of specific frequency regions from each ear were obtained (LSM5; Zeiss) using a high-resolution, water-immersion objective (C-Apochromat 63 \times , 1.20 numerical aperture). For whole mounts, each stack spanned 80–100 μm of cochlear length and two adjacent stacks were imaged at each locus. Image stacks were processed using Volocity software (Improvision, 4.x; PerkinElmer Life and Analytical Sciences).

Results

To test our hypothesis that Ocm plays a pivotal role in OHC function, we created a mutant mouse in which the Ocm gene was targeted for deletion. Our targeting strategy removed exons 2–4 of the Ocm gene (Fig. 1A). Exons 3 and 4 contain two Ca^{2+} binding motifs (Henzl et al., 2000), and exon 2 contains the N terminus of Ocm. Germ-line transmission was confirmed initially by Southern blot analysis (Fig. 1B) and then subsequently by a multistep PCR scheme involving both a 5' Lox P site and a 3' cassette and/or 3' Lox P site. Crossing the *Ocm*^{flox/flox} mice to mice with β -actin-Cre-driven promoter expression generated *Actb*^{Cre}; *Ocm*^{flox/flox} mice. These *Actb*^{Cre}; *Ocm*^{flox/flox} mice are essentially *Ocm*^{-/-} mice as verified by RT-PCR (data not shown) and the lack of Ocm immunoreactivity (IR; Fig. 1C,D). For immunoreactivity, we tested both a monoclonal mouse anti-Ocm and a polyclonal rabbit anti-Ocm, both of which were raised against recombinant full-length Ocm (Simmons et al., 2010). In age-matched controls, the Ocm antisera labeled OHCs throughout the cochlear spiral as expected. There was no Ocm labeling in tissues from *Ocm*^{-/-} mutants with either antibody (Fig. 1C,D). Although IHCs routinely labeled for α -parvalbumin (Fig. 1C,D) and calretinin (data not shown) in adult *Ocm*^{-/-} mutants and wild-type controls, there was no labeling of either protein in *Ocm*^{-/-} OHCs from basal locations, suggesting that expression was not altered for either of these Ca^{2+} buffers. Furthermore, *Ocm*^{-/-} mutants show normal developmental expression of α -parvalbumin and hair bundles in IHCs and OHCs from postnatal day (P) 4 (Fig. 1E) up to 4 weeks. None of the *Ocm*^{-/-} mutants had any obvious behavioral or developmental abnormalities and no difference in body weights compared with wild-type littermates.

To test cochlear function, we measured ABRs in anesthetized adult mice between aged 14–26 weeks using seven test frequencies (5.6, 8, 11.3, 16, 22.4, 32, and 45.2 kHz). As shown in Figure 1F, average ABR wave responses to a 16 kHz tone at the highest sound pressure level (80 dB SPL) are similar for wild-type and heterozygous mice but absent for *Ocm*^{-/-} mice. In wild-type mice, ABR thresholds vary with frequency from a sound pressure level as low as 35 dB at 11.3 kHz to as high as 65 dB at 45.6 kHz (Fig. 1G). *Ocm*^{-/-} mutants were profoundly hearing impaired at this young-adult age, with ABR thresholds 20–50 dB higher than those in wild-type mice, corresponding to what would be considered a moderate-to-severe hearing loss in humans. In *Ocm*^{-/-} mutants, the lowest measurable ABR thresholds were at the lowest test frequencies: 77.8 dB SPL at 5.7 kHz and 82.8 dB SPL at 8 kHz. Heterozygous mice show ABR thresholds similar to their wild-type counterparts; the small differences in the mean values were not statistically significant ($p = 0.20$ by two-way ANOVA).

To assess OHC function *in vivo*, we measured DPOAEs, the electromechanical distortions in response to two primary tones (f_1 and f_2) that are amplified by OHCs and propagated back through the middle ear. In the *Ocm*^{-/-} mutant at 14–26 weeks, DPOAE thresholds were at or near the measurement ceiling for all test frequencies (Fig. 1H), consistent with a defective OHC or

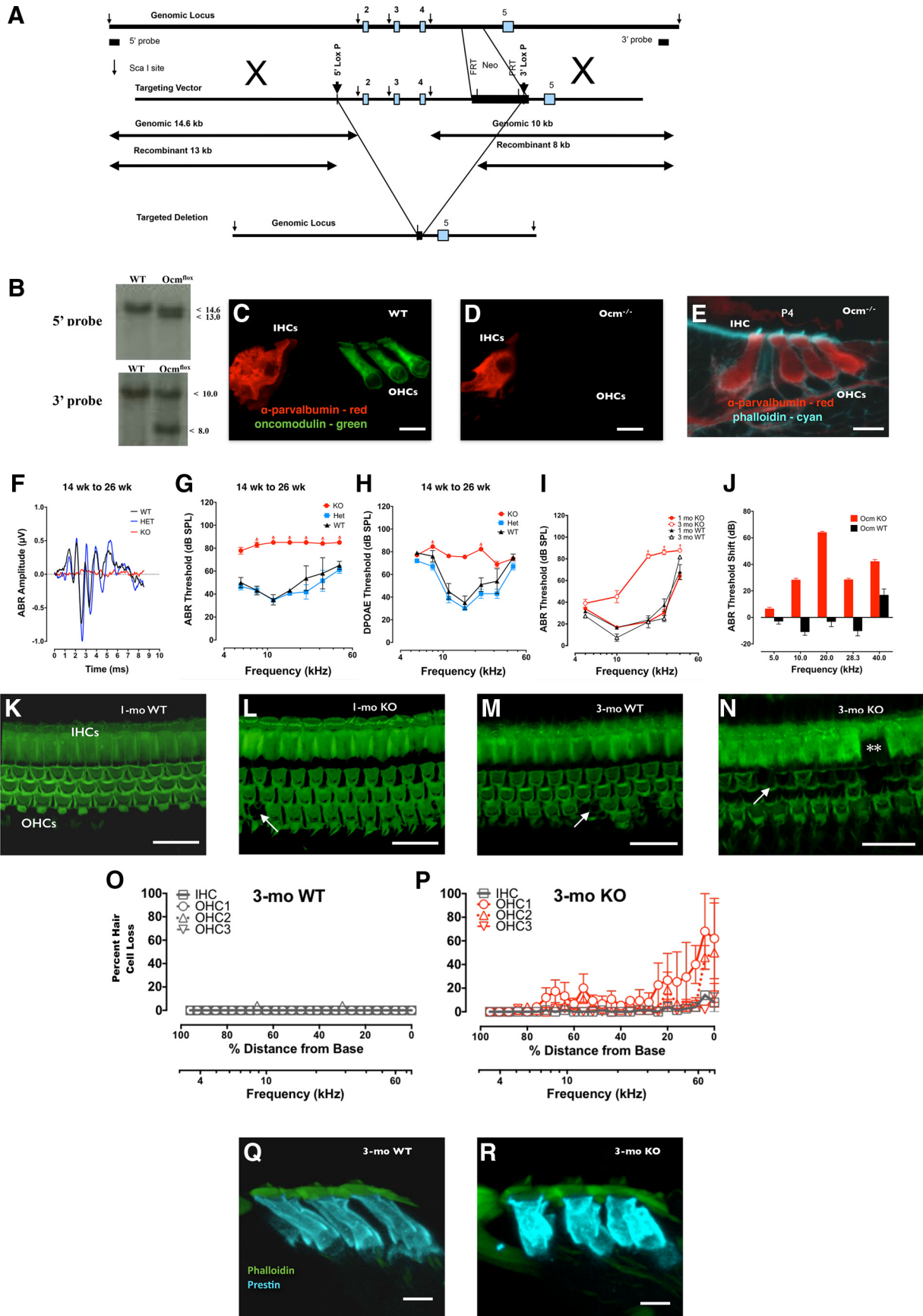


Figure 1. *A*, Schematic illustrating the strategy used for targeted conditional deletion of *Ocm*. A *LoxP* site was engineered 5' of exon 2, and an *Flp*–*neo*–*Flp*–*LoxP* cassette was engineered 3' of exon 4. *B*, Southern blots of genomic DNA from wild-type and *Ocm^{flx}* using a 5' and 3' probe and *Sca*I digestion. *C*, Cross-section from the basal turn of a wild-type cochlea at 1 month shows *Ocm* immunolabeling (green) in OHCs but not IHCs. α -Parvalbumin (red) labels IHCs but not OHCs. Scale bars, 10 μ m. *D*, Basal turn section from an *Ocm^{-/-}* cochlea shows no *Ocm* immunolabeling in OHCs. Scale bars, 10 μ m. *E*, Basal turn section from a *Ocm^{-/-}* cochlea at postnatal day 4 (P4) shows α -parvalbumin (red) and phalloidin (cyan) labeling. Scale bars, 10 μ m. *F*, ABR amplitude vs time for 14-week-old wild-type (black), heterozygous (blue), and homozygous (red) mice. *G*, ABR threshold vs frequency for 14-week-old wild-type (black triangles), heterozygous (blue squares), and homozygous (red circles) mice. *H*, DPOAE threshold vs frequency for 14-week-old wild-type (black triangles), heterozygous (blue squares), and homozygous (red circles) mice. *I*, ABR threshold vs frequency for 1-month-old (red circles) and 3-month-old (red squares) homozygous mice and 1-month-old (black triangles) and 3-month-old (black diamonds) wild-type mice. *J*, ABR threshold shift vs frequency for 1-month-old (red bars) and 3-month-old (black bars) homozygous mice. *K*, *L*, IHCs and OHCs in 1-month-old wild-type (K) and homozygous (L) mice. Arrow in *L* points to OHC loss. *M*, *N*, IHCs and OHCs in 3-month-old wild-type (M) and homozygous (N) mice. Arrow and asterisks (***) in *N* point to OHC loss. *O*, *P*, Percent hair cell loss vs distance from base vs frequency for 3-month-old wild-type (O) and homozygous (P) mice. Legend: IHC (open circles), OHC1 (open squares), OHC2 (open triangles), OHC3 (open diamonds). *Q*, *R*, Phalloidin (green) and Prestin (cyan) staining in 3-month-old wild-type (Q) and homozygous (R) mice. Scale bars, 10 μ m.

cochlear amplification system (Mills 2006). These results suggest that the expression of Ocm is critical for cochlear function.

We also investigated the onset of cochlear dysfunction in *Ocm*^{-/-} mutants. Figure 1I shows ABR thresholds for *Ocm*^{-/-} mutants and wild types at two different ages using five test frequencies: 5, 10, 20, 28.3, and 40 kHz. At 4 weeks, 2 weeks after hearing onset, ABR thresholds were similar between the two genotypes (Fig. 1I). The slight differences at middle frequencies were not statistically significant ($p = 0.11$ by two-way ANOVA). However, by 12 weeks, *Ocm*^{-/-} mutants showed elevated ABR thresholds above 10 kHz when compared with 4 weeks. The differences in threshold responses between 4 and 12 weeks were replotted as threshold shifts (Fig. 1J). In *Ocm*^{-/-} mutants, threshold shifts ranged from as little as 6 dB at 5 kHz to as much as 60 dB at 20 kHz. In contrast, wild types at 12 weeks showed little change from 4 weeks.

In *Ocm*^{-/-} mutants up to 8 weeks, OHC morphology and prestin-IR (data not shown) were normal with minimal hair cell loss throughout the cochlear spiral (Fig. 1K,L). However, after 12 weeks, *Ocm*^{-/-} mutants showed greater scattered OHC loss and scattered loss of pillar cells (Fig. 1N,P), especially in higher-frequency regions compared with wild-type controls (Fig. 1M,O). In *Ocm*^{-/-} mutants, OHC loss was spotty, with alternating regions of intact and missing cells. The degree of loss was variable across animals but generally greatest in rows 1 and 2 and least in row 3. IHC loss was minimal but significantly different from control at 12 weeks in the extreme base of the cochlea. These results suggest that Ocm may have a modulatory effect on the mechanoelectric transduction or prestin-driven electromotive processes. Because we could find no obvious differences in phalloidin-stained bundles between wild-type and *Ocm*^{-/-} mutant OHCs at 3 months, we compared prestin-IR in wild types (Fig. 1Q) and *Ocm*^{-/-} mutants (Fig. 1R). At 2 months, there were no obvious differences in prestin-IR between wild-type controls and *Ocm*^{-/-} mutant mice. However, at 3 months, unlike wild-type control OHCs, prestin-labeled *Ocm*^{-/-} OHCs from middle-frequency regions appear shorter and more intensely labeled, suggesting that Ocm and/or Ca²⁺ buffering help maintain normal prestin expression patterns.

Discussion

In the present study, we assessed the role of Ocm, an EF-hand Ca²⁺-binding protein predominately expressed in OHCs in the

←

(Figure legend continued.) mutant cochlea shows no Ocm (green) or α -parvalbumin (red) immunolabeling in OHCs. IHCs do show immunoreactivity for α -parvalbumin (red). **E**, Basal turn section from an *Ocm*^{-/-} mutant at P4. α -Parvalbumin (red) labels both IHCs and OHCs. Phalloidin (cyan) staining is also shown. **F**, Averaged ABR wave responses from adult (14–26 weeks) wild-type ($n = 3$), heterozygous ($n = 6$), and *Ocm*^{-/-} mutant ($n = 5$) mice to 16 kHz tone bursts given at 80 dB SPL. **G**, Mean ABR thresholds for adult (14–26 weeks) *Ocm*^{-/-} mutants ($n = 8$), Ocm heterozygotes ($n = 8$), and wild-type mice ($n = 4$). **H**, Mean \pm SEM DPOAE thresholds as a function of f_f , frequency from the same mice as in **G**. Small arrows indicate DPOAEs were at the measurement ceiling at which the acoustic system creates its own distortions. **I**, Mean ABR thresholds in 4-week-old *Ocm*^{-/-} mutants (red filled circles, $n = 26$) and wild types (black filled squares, $n = 14$) compared with 12-week-old *Ocm*^{-/-} mutants (red open circles, $n = 4$) and wild types (black open squares, $n = 5$). **J**, Mean \pm SEM ABR threshold shifts in 3-month-old mutants ($n = 4$) and wild types ($n = 5$) compared with 4-week-old wild types, as in **I**. **K–N**, Confocal images of the organ of Corti stained with phalloidin. All images are from the 45 kHz region in *Ocm*^{-/-} mutants (**L, M**) and wild types (**K, N**) at 1 and 3 months. Arrows denote missing hair cells. Asterisks denote missing pillar cells. Scale bars, 30 μ m. **O, P**, Mean \pm SEM hair cell loss at 3 months from wild-type ($n = 3$) and mutant ($n = 3$) cochleae. **Q**, In wild-type controls, prestin (cyan) labels the lateral membrane of OHCs and phalloidin (green) stains actin. **R**, In *Ocm*^{-/-} mutants (KO) at 3 months, OHCs are shorter and more intensely labeled than in corresponding middle-to-apical regions of the wild-type cochlea. Scale bars: **Q**, **R**, 10 μ m.

mammalian cochlea. We generated a conditional knock-out line using Cre-recombinase driven by the β -actin promoter (*Actb*^{Cre}; *Ocm*^{fllox/fllox}). Using this targeted deletion of Ocm, we show that lack of this Ca²⁺ buffer leads to progressive cochlear dysfunction beginning after 1 month and results in ABR threshold shifts and loss of DPOAEs by 4 months of age. Functionally, the absence of Ocm mimics an accelerated aging or noise damage process. The presence of normal ABR and DPOAE thresholds in *Ocm*^{-/-} mutants at 1 month shows that Ocm is not essential for the development of cochlear function. However, the progressive hearing loss after 1 month suggests that Ocm expression critically protects OHCs from damage in the mature ear.

In hair cells, Ca²⁺ is both a primary and a secondary messenger. Calcium serves as a primary ion for at least four different channel types found in OHCs (Sziklai 2004; Fettiplace 2006). Calcium can also be released from the subsurface cisternae and mitochondria in an IP₃-dependent manner (Frolokov et al., 2000; Szönyi et al., 2001). Calcium entering through nicotinic receptors acts as a second messenger by binding the SK2 channel, which results in an outflow of potassium (Oliver et al., 2000; Marcotti et al., 2004). Calcium can also bind to calmodulin activating many calmodulin-dependent pathways (Sziklai et al., 2001; Farahbakhsh and Narins 2006). Ca²⁺ buffers play an important role in regulating intracellular Ca²⁺ concentration, and excess Ca²⁺ can lead to cell death (Rizzuto et al., 2003).

Given the presumed importance of EF-hand Ca²⁺-binding proteins such as α -parvalbumin, calbindin-D28k, and calretinin in hair cells, genetic disruption of these Ca²⁺ buffers should affect auditory function. However, a recent study of a triple knock-out of these EF-hand mobile buffers found that there was little or no loss of hearing in 12–16 week old mutants (Pangršič et al., 2015), suggesting that hair cells have strong compensatory mechanisms to regulate Ca²⁺ at least up through the ages tested. Because the onset of Ocm expression coincides with a decline in the expression of other EF-hand Ca²⁺ buffers in OHCs, the loss of Ocm might lead to upregulation of these Ca²⁺ buffers. However, previous studies of genetic disruption of EF-hand Ca²⁺ buffers suggest that each Ca²⁺ buffer has distinct properties and that their absence in knock-out mice cannot be simply substituted by another EF-hand family member (Chen et al., 2006; Schwaller 2012). For example, in α -parvalbumin-deficient mice, the major compensatory changes observed are altered dendritic morphology and changes in mitochondria size and location but not changes in expression of other EF-hand Ca²⁺ buffers (Schwaller 2012). Consistent with this idea, we did not find any changes in the immunoreactivity of other EF-hand Ca²⁺ buffers in OHCs. We know that Ca²⁺ levels in hair cells can be regulated by pumps, such as by the plasma membrane Ca²⁺ ATPase (PMCA), Na⁺/Ca²⁺ exchanger (NCX), sarcoplasmic/endoplasmic reticulum Ca²⁺ ATPase (SERCA), and by a uniporter into mitochondria (Sziklai 2004). Thus, the lack of EF-hand Ca²⁺ buffers may be compensated for by increased mitochondrial Ca²⁺ uptake or increased PMCA activity. However, none of these were sufficient to compensate for the loss of Ocm, suggesting a functionally distinctive role.

In OHCs, Ocm may have a dual role as a Ca²⁺ buffer and sensor similar to suggested roles for calmodulin (Schwaller 2009). As a buffer, Ocm may help to titrate or isolate release of Ca²⁺ from the subsurface cisternae. Increases in intracellular Ca²⁺ lead to a decrease in axial stiffness and trigger Ca²⁺-dependent slow motility (Mammano 2011). Alternatively, as a Ca²⁺ sensor, Ocm may mediate the activation of Ca²⁺/calmodulin-dependent phosphorylation of cytoskeletal proteins

and/or prestin, leading to changes in OHC stiffness and subsequently changes to motor function (Frolenkov et al., 2003; Sziklai 2004). In the present study, the lack of Ocm also leads to abnormal prestin expression. However, this abnormal expression occurs after elevated thresholds were observed. Abnormal prestin expression in *Ocm*^{-/-} mutants again raises the possibility that Ocm and prestin are somehow linked. Indeed, previous reports link Ocm with prestin because both are downregulated by mutations in microRNA-96 that give rise to a progressive hearing loss phenotype (Lewis et al., 2009). Previous studies have proposed that Ca²⁺-based phosphorylation mechanisms affect the gain and magnitude of electromotility (Dulon et al., 1991; Sziklai et al., 2001; Stepanyan and Frolenkov 2009). Ocm is preferentially localized to the base of the hair bundle and to the basolateral membrane of OHCs (Simmons et al., 2010), a labeling pattern similar to proteins involved in Ca²⁺-dependent processes that affect the motor function of OHCs, such as CaMKIV and prestin. Phosphorylation of both cytoskeletal and prestin proteins is modulated by intracellular Ca²⁺. We conclude that Ocm has a distinctive function among endogenous Ca²⁺ buffers. It is possible that Ocm helps maintain OHC-based electromotility and the long-term survival of OHCs.

References

- Airaksinen L, Virkkala J, Aarnisalo A, Meyer M, Ylikoski J, Airaksinen MS (2000) Lack of calbindin-D28k does not affect hearing level or survival of hair cells in acoustic trauma. *ORL J Otorhinolaryngol Relat Spec* 62:9–12. [CrossRef Medline](#)
- Chen G, Racay P, Bichet S, Celio MR, Egli P, Schwaller B (2006) Deficiency in parvalbumin, but not in calbindin D-28k upregulates mitochondrial volume and decreases smooth endoplasmic reticulum surface selectively in a peripheral, subplasmalemmal region in the soma of Purkinje cells. *Neuroscience* 142:97–105. [CrossRef Medline](#)
- Dulon D, Zajic G, Schacht J (1991) Differential motile response of isolated inner and outer hair cells to stimulation by potassium and calcium ions. *Hear Res* 52:225–231. [CrossRef Medline](#)
- Farahbakhsh NA, Narins PM (2006) Slow motility in hair cells of the frog amphibian papilla: Ca²⁺-dependent shape changes. *Hear Res* 212:140–159. [CrossRef Medline](#)
- Fettiplace R (2006) Active hair bundle movements in auditory hair cells. *J Physiol* 576:29–36. [CrossRef Medline](#)
- Fridberger A, Flock A, Ulfendahl M, Flock B (1998) Acoustic overstimulation increases outer hair cell Ca²⁺ concentrations and causes dynamic contractions of the hearing organ. *Proc Natl Acad Sci U S A* 95:7127–7132. [CrossRef Medline](#)
- Frolenkov GI, Mammano F, Belyantseva IA, Coling D, Kachar B (2000) Two distinct Ca²⁺-dependent signaling pathways regulate the motor output of cochlear outer hair cells. *J Neurosci* 20:5940–5948. [Medline](#)
- Frolenkov GI, Mammano F, Kachar B (2003) Regulation of outer hair cell cytoskeletal stiffness by intracellular Ca²⁺: underlying mechanism and implications for cochlear mechanics. *Cell Calcium* 33:185–195. [CrossRef Medline](#)
- Hackney CM, Mahendrasingam S, Penn A, Fettiplace R (2005) The concentrations of calcium buffering proteins in mammalian cochlear hair cells. *J Neurosci* 25:7867–7875. [CrossRef Medline](#)
- Henzl MT, Larson JD, Agah S (2000) Influence of monovalent cations on rat alpha- and beta-parvalbumin stabilities. *Biochemistry* 39:5859–5867. [CrossRef Medline](#)
- Lewis MA, Quint E, Glazier AM, Fuchs H, De Angelis MH, Langford C, van Dongen S, Abreu-Goodger C, Piipari M, Redshaw N, Dalmay T, Moreno-Pelayo MA, Enright AJ, Steel KP (2009) An ENU-induced mutation of miR-96 associated with progressive hearing loss in mice. *Nat Genet* 41:614–618. [CrossRef Medline](#)
- Lewit-Bentley A, Réty S (2000) EF-hand calcium-binding proteins. *Curr Opin Struct Biol* 10:637–643. [CrossRef Medline](#)
- MacManus JP, Watson DC, Yaguchi M (1983) A new member of the troponin C superfamily: comparison of the primary structures of rat oncomodulin and rat parvalbumin. *Biosci Rep* 3:1071–1075. [CrossRef Medline](#)
- Maison SF, Liu XP, Eatock RA, Sibley DR, Grandy DK, Liberman MC (2012) Dopaminergic signaling in the cochlea: receptor expression patterns and deletion phenotypes. *J Neurosci* 32:344–355. [CrossRef Medline](#)
- Mammano F (2011) Ca²⁺ homeostasis defects and hereditary hearing loss. *BioFactors* 37:182–188. [CrossRef Medline](#)
- Marcotti W, Johnson SL, Kros CJ (2004) A transiently expressed SK current sustains and modulates action potential activity in immature mouse inner hair cells. *J Physiol* 560:691–708. [CrossRef Medline](#)
- Mills DM (2006) Determining the cause of hearing loss: differential diagnosis using a comparison of audiometric and otoacoustic emission responses. *Ear Hear* 27:508–525. [CrossRef Medline](#)
- Ohlemiller KK, Rybak Rice ME, Rellinger EA, Ortmann AJ (2011) Divergence of noise vulnerability in cochleae of young CBA/J and CBA/CaJ mice. *Hear Res* 272:13–20. [CrossRef Medline](#)
- Oliver D, Klöcker N, Schuck J, Baukrowitz T, Ruppersberg JP, Fakler B (2000) Gating of Ca²⁺-activated K⁺ channels controls fast inhibitory synaptic transmission at auditory outer hair cells. *Neuron* 26:595–601. [CrossRef Medline](#)
- Pack AK, Slepecky NB (1995) Cytoskeletal and calcium-binding proteins in the mammalian organ of Corti: cell type-specific proteins displaying longitudinal and radial gradients. *Hear Res* 91:119–135. [CrossRef Medline](#)
- Pangršič T, Gabrielaitis M, Michanski S, Schwaller B, Wolf F, Strenzke N, Moser T (2015) EF-hand protein Ca²⁺ buffers regulate Ca²⁺ influx and exocytosis in sensory hair cells. *Proc Natl Acad Sci U S A* 112:E1028–E1037. [CrossRef Medline](#)
- Rizzuto R, Pinton P, Ferrari D, Chami M, Szabadkai G, Magalhães PJ, Di Virgilio F, Pozzan T (2003) Calcium and apoptosis: facts and hypotheses. *Oncogene* 22:8619–8627. [CrossRef Medline](#)
- Sage C, Ventéo S, Jeromin A, Roder J, Dechesne CJ (2000) Distribution of frequenin in the mouse inner ear during development, comparison with other calcium-binding proteins and synaptophysin. *Hear Res* 150:70–82. [CrossRef Medline](#)
- Schwaller B (2009) The continuing disappearance of “pure” Ca²⁺ buffers. *Cell Mol Life Sci* 66:275–300. [CrossRef Medline](#)
- Schwaller B (2012) The use of transgenic mouse models to reveal the functions of Ca(2+) buffer proteins in excitable cells. *Biochim Biophys Acta* 1820:1294–1303. [CrossRef Medline](#)
- Simmons DD, Tong B, Schrader AD, Hornak AJ (2010) Oncomodulin identifies different hair cell types in the mammalian inner ear. *J Comp Neurol* 518:3785–3802. [CrossRef Medline](#)
- Staubli F, Klein A, Rentsch JM, Hameister H, Berchtold MW (1995) Structure and chromosomal localization of the mouse oncomodulin gene. *Mamm Genome* 6:769–777. [CrossRef Medline](#)
- Stepanyan R, Frolenkov GI (2009) Fast adaptation and Ca²⁺ sensitivity of the mechanotransducer require myosin-XVa in inner but not outer cochlear hair cells. *J Neurosci* 29:4023–4034. [CrossRef Medline](#)
- Sziklai I (2004) The significance of the calcium signal in the outer hair cells and its possible role in tinnitus of cochlear origin. *Eur Arch Otorhinolaryngol* 261:517–525. [CrossRef Medline](#)
- Sziklai I, Szönyi M, Dallos P (2001) Phosphorylation mediates the influence of acetylcholine upon outer hair cell electromotility. *Acta Otolaryngol* 121:153–156. [CrossRef Medline](#)
- Szönyi M, He DZ, Ribári O, Sziklai I, Dallos P (2001) Intracellular calcium and outer hair cell electromotility. *Brain Res* 922:65–70. [CrossRef Medline](#)
- Thalmann I, Thalmann R, Henzl MT (1998) Novel calcium sensor in the outer hair cells: quantitation of oncomodulin. *Primary Sensory Neuron* 2:283–296. [CrossRef](#)
- Wassarman KM, Lewandoski M, Campbell K, Joyner AL, Rubenstein JL, Martinez S, Martin GR (1997) Specification of the anterior hindbrain and establishment of a normal mid/hindbrain organizer is dependent on Gbx2 gene function. *Development* 124:2923–2934. [Medline](#)
- Yang D, Thalmann I, Thalmann R, Simmons DD (2004) Expression of alpha and beta parvalbumin is differentially regulated in the rat organ of corti during development. *J Neurobiol* 58:479–492. [CrossRef Medline](#)
- Yin Y, Cui Q, Gilbert HY, Yang Y, Yang Z, Berlinicke C, Li Z, Zaverucha-doValle C, He H, Petkova V, Zack DJ, Benowitz LI (2009) Oncomodulin links inflammation to optic nerve regeneration. *Proc Natl Acad Sci U S A* 106:19587–19592. [CrossRef Medline](#)
- Zhang M, Kalinec GM, Urrutia R, Billadeau DD, Kalinec F (2003) ROCK-dependent and ROCK-independent control of cochlear outer hair cell electromotility. *J Biol Chem* 278:35644–35650. [CrossRef Medline](#)